Atomistic Brownian Dynamics Simulation of Peptide Phosphorylation

Tongye Shen,*,† Chung F. Wong,‡ and J. Andrew McCammon‡,§

Contribution from the Department of Physics, Howard Hughes Medical Institute and Department of Pharmacology, Department of Chemistry and Biochemistry, University of California, San Diego, La Jolla, California 92093-0365

Received January 23, 2001. Revised Manuscript Received May 14, 2001

Abstract: We report the implementation of an all-atom Brownian dynamics simulation model of peptides using the constraint algorithm LINCS. The algorithm has been added as a part of UHBD. It uses adaptive time steps to achieve a balance between computational speed and stability. The algorithm was applied to study the effect of phosphorylation on the conformational preference of the peptide Gly-Ser-Ser-Ser. We find that the middle serine residue experiences considerable conformational change from the C_{7eq} to the α_R structure upon phosphorylation. NMR ^3J coupling constants were also computed from the Brownian trajectories using the Karplus equation. The calculated ^3J results agree reasonably well with experimental data for phosphorylated peptide but less so for doubly charged phosphorylated one.

I. Introduction

Molecular dynamics (MD) simulations of biomolecules[1] provide detailed atomistic information that is often difficult to obtain directly from experiments. However, it is difficult to carry out long simulations for long polypeptides with explicit solvent models. Salt effects are also difficult to include by simply adding counterions to the simulation since it takes a long time for the ions to thoroughly sample the important space around a polypeptide. Stochastic dynamics simulations provide a potentially useful tool for simulating the long-time dynamics of polypeptides. In a Langevin dynamics (LD) simulation, one does not include the solvent molecules and the counterions explicitly but models their effects implicitly by using solvent-averaged, frictional, and stochastic forces. The Langevin equation can be solved more easily in the overdamped limit, at which inertial effects are ignored. This approximation usually applies to studying the lower-frequency dynamics of polypeptides, for example, when the bond vibrations of the polypeptides are neglected. In this paper, we term the overdamped limit of Langevin dynamics as Brownian dynamics (BD).

Earlier BD simulations of polypeptides modeled[2] a polypeptide as a string of spheres, each representing an amino acid, connected successively by virtual bonds. As computer power is increasing, more detailed BD models have also been introduced. These include models with each residue represented by two spheres (one represents the backbone and the other the side chain)[3] and atomistic models.[4] For these detailed models, efficient and stable algorithms for maintaining bond-length constraints are needed. The SHAKE algorithm[5] commonly used in MD simulations is not adequate for BD simulations because the time steps in the latter simulations are larger and the SHAKE algorithm fails to converge. Here we describe the implementation of a full atomistic BD algorithm into UHBD[6] using the constraint technique LINCS.[7] We test this algorithm by using it to study the conformational switching of the peptide Gly-Ser-Ser-Ser (GSSS) upon phosphorylation.

II. Methods

A. BD Algorithm. The LD equation can be expressed as

$$m_i \frac{\mathrm{d}^2 \vec{r}_i}{\mathrm{d}t^2} = -\xi_i \frac{\mathrm{d}\vec{r}_i}{\mathrm{d}t} + (\vec{f}_i(\vec{r}_i) + \vec{R}_i(t)) \tag{1}$$

Here index i labels particle i in the system, and the total force consists of three parts. In addition to the systematic forces given by the negative gradient of the potential of mean force, $\vec{f}_i = -\nabla_i U(\{\vec{r}_j\})$, there are frictional and stochastic forces to describe the dynamical effects of the solvent on the system. $\vec{R}_i(t)$ is a random force having a zero mean $\langle \vec{R}(t) \rangle = 0$ and a variance $\langle \vec{R}_i(t)\vec{R}_j(0) \rangle = 2\xi_{ij}k_BT\delta(t)$. In this work, we neglect hydrodynamic interactions so that the frictional matrix is diagonal, that is, $\xi_{ij} = \delta_{ij}\xi_i$ in which ξ_i is a frictional coefficient. The collision frequency γ_i is defined as ξ_i/m_i.

In the overdamped limit, we set the left side of eq 1 to zero. Integrating the resulting equation for a time step of dt gives the following equation for propagating a Brownian trajectory:

$$\mathrm{d}\vec{r}_i = \frac{D_i}{k_BT}\vec{f}_i \mathrm{d}t + \sqrt{2D_i \mathrm{d}t}\,\vec{\omega}_i, \tag{2}$$

where $D_i = k_BT/\xi_i$ is the diffusion coefficient and $\vec{\omega}_i$ is a random noise vector obtained from a standard normal distribution. Equation 2 is the first-order Ermak−McCammon algorithm.[8] Later, several higher-order algorithms such as the stochastic Runge−Kutta (SRK)[9] and the stochastic expansion (SE)[10] algorithms were developed, and these

* To whom correspondence should be addressed. E-mail: tshen@ucsd.edu.

† Department of Physics.

‡ Howard Hughes Medical Institute and Department of Pharmacology.

§ Department of Chemistry and Biochemistry.

(1) McCammon J. A.; Harvey, S. C. *Dynamics of Proteins and Nucleic Acids*; Cambridge University Press: Cambridge, 1987.

(2) McCammon, J.; Northrup, S. H.; Karplus, M.; Levy, R. M. *Biopolymers* **1980**, *19*, 2033−2045.

(3) Takada, S.; Luthey-Schulten, Z.; Wolynes, P. G. *J. Chem. Phys.* **1999**, *110*, 11616−11629.

(4) Gronbech-Jensen, N.; Doniach, S. *J. Comput. Chem.* **1994**, *15*, 997−1012.

(5) Ryckaert, J. P.; Ciccotti, G.; Berendsen, H. J. C. *J. Comput. Phys.* **1977**, *23*, 327−341.

(6) Davis, M. E.; Madura, J. D.; Luty, B. A.; McCammon, J. A. *Comput. Phys. Commun.* **1991**, *62*, 187−197.

(7) Hess, B.; Bekker, H.; Berendsen, H. J. C.; Fraaije, J. G. *J. Comput. Chem.* **1997**, *18*, 1463−1472.

(8) (a) Ermak, D. L. *J. Chem. Phys.* **1975**, *62*, 4189−4196. (b) Ermak, D. L.; McCammon, J. A. *J. Chem. Phys.* **1978**, *69*, 1352−1360.

(9) Honeycutt, R. L. *Phys. Rev. A* **1992**, *45*, 600−603.

(10) Greiner, A.; Strittmatter, W.; Honerkamp, J. *J. Stat. Phys.* **1988**, *51*, 95−108.

10.1021/ja010190t CCC: $20.00
Published on Web 08/21/2001

algorithms had been compared using a simple homogeneous system.[11] We have tested the SRK scheme and several others and found that the time step could not be increased much by these higher-order algorithms for polypeptides. These algorithms also require several expensive evaluations of forces or their time derivatives each time step, and we decided to use a simpler first-order algorithm in this work.

B. Constraints. By eliminating the less interesting high-frequency motions such as those arising from bond vibrations, one can use larger time steps in BD simulations. In this study, we constrain *all* of the bond lengths of the tetrapeptide to make it easier to simulate the system to the microsecond time scale. Here, we use the LINCS[7] algorithm for imposing bond-length constraints. LINCS is a predictor−corrector algorithm that has been demonstrated[12] to be more efficient and stable than the well-known SHAKE algorithm.[5] It is also easier to parallelize LINCS than SHAKE. We do not constrain bond angles since previous dynamical simulations have demonstrated[13,14] coupling between angular and lower frequency motion.

C. Adaptive Time Step. Constraining bond lengths makes it possible to use larger time steps in BD simulations, but we found unfavorable atomic clashes can occur once in millions of steps when a large time step was used. These are likely due to the fact that constraint algorithm only regulates the bonding terms for filtering out high frequency modes, but does not include the nonbonding terms, especially the van der Waals (vdW) interaction.

To avoid this problem without sacrificing the use of large time steps, we introduced an adaptive time step method into the algorithm. Adaptive stepsize has been widely used in numerical integration of differential equations,[15] and the determination of stepsize is usually obtained from error analysis. Our algorithm dynamically chooses a time step based on analysis of the energy of a polypeptide during a BD simulation.

The algorithm applies a user-chosen "normal" time step dt most of the time. However, the time step was split into n smaller ones dt' = dt/n whenever the vdW energy of a configuration is larger than a predetermined threshold. That is, the code will decide the size of the next time step base on the vdW energy of the previous step. The proper threshold and normal time step are system-, model-, and temperature-dependent. Generally the more detailed the model, the smaller the time step one must use. For the tetrapeptide studied here, the threshold is of the order of tens of kcal/mol and dt is about 10 fs. The small time steps are used less than 1% of the time in our simulations. This adaptive time step approach permits a time step dt to be several times larger than that in a constant time step algorithm.

D. All-Atom Model and Parametrization. The CHARMM all-atom force field[16] was used in the simulation. Solvent-screening effects were modeled by using a distance-dependent dielectric function with $\epsilon = R$. Hydrophobic effects were modeled[17] by a term proportional to the solvent accessible surface (SAS) area of the polypeptide. The proportionality constant, microscopic surface tension, was set at 6 cal $(mol \cdot Å^2)^{-1}$.

The diffusion coefficients of individual atoms were assigned according to

$$D_i = w_i \cdot \frac{k_B T^*}{6\pi\eta(r_i + 1.4Å)} \tag{3}$$

Here, T^* is 300 K and η is the viscosity of water: 0.891 cp. The weighting factor w_i was chosen according to

$$w_i = \begin{Bmatrix} 2.5 & \text{hydrogens,} \\ 1 & \text{others} \end{Bmatrix} \tag{4}$$

This is essentially the Stokes−Einstein equation with the radius of each atom chosen as its vdW radius plus 1.4 Å, the approximate radius of a water molecule. Light atoms were given a weight w_i to increase their diffusion coefficients. This was done to make the simulation parameters closer to an earlier simulation employing a fixed collision frequency γ for all atoms.[18] However, the choice of diffusion coefficients only affects (assuming that all diffusion coefficients are larger than 0) dynamical properties, not static properties as those calculated in this paper.

III. Peptide Phosphorylation

Protein phosphorylation plays an important role in metabolic regulation.[19] Significant efforts have been devoted to investigate whether phosphorylation triggers signal transduction by altering the conformation of a protein and, if so, whether the conformational change results from tertiary interaction alone or from secondary interaction as well. By simulating short peptides, one can minimize the effects of tertiary interactions and focus on analyzing secondary ones. Here, we use our atomistic BD simulation algorithm to simulate the conformational distribution of a tetrapeptide GSSS in the phosphorylated and nonphosphorylated forms to gain insights into the switching of secondary structure by protein phosphorylation.

A key reason for choosing this tetrapeptide is that it has been studied by NMR experiments both in the phosphorylated and nonphosphorylated form.[20] The proton chemical shifts and the spin−spin coupling constants of the protons in $HNC_\alpha Hs$ have been measured for the unphosphorylated peptide, GSSS, and the peptide with the middle serine phosphorylated, Gly-Ser-Ser(p)-Ser (GSSpS). The NMR data suggest that phosphorylation induces backbone conformational changes.

A total of five peptides were built with Quanta98.[21] They are listed in Table 1. They differ from each other by whether their termini are blocked and whether the middle serines are phosphorylated. We used acetyl ($CH_3C{=}O$) and methylamide ($NHCH_3$) to block the amino and carboxy termini, respectively, for the blocked peptides. Note that our carboxy termini were blocked *differently* from the experimental study[20] in which NH_2 was used instead of methylamide. The pK_a's[22] of the phosphoryl group (pK_{a1} < 2 and pK_{a2} = 5.9) suggest that the terminally blocked phosphorylated peptides exist largely in the totally deprotonated (dianionic) form at pH 7 or higher. However, at lower pHs such as those used in the experimental study of GSSS,[20] the population of both the totally deprotonated (b2, $-2e$) and the singly protonated (b1 and z1, $-1e$) forms are significant. Figure 1 shows a structure of b2.

The initial structures of the peptides were built in the fully extended form and all-atom models were used. The CHARMM force field[16] only has potential parameters for the singly protonated phosphoserine. In modeling the doubly charged phosphoserine, we deleted the hydrogen of the singly protonated form and recalculated the atomic charges using the Gasteiger method.[23]

(11) (a) Branka, A. C.; Heyes, D. M. *Phys. Rev. E.* **1999**, *60*, 2381−2387. (b) *ibid.* **1998**, *58*, 2611−2615.
(12) *GROMACS*, ver. 2.0; http://rugmd0.chem.rug.nl/~gmx.
(13) Hinsen, K.; Kneller, G. R. *Phys. Rev. E.* **1995**, *52*, 6868−6874.
(14) van Gunsteren, W. F.; Karplus, M. *Macromolecules* **1982**, *15*, 1528−1544.
(15) Press: W. H.; Teukolsky, S. A.; Vetterling, W. T.; Flannery, B. P. *Numerical Recipe in Fortran 77*; Cambridge University Press: New York, 1992.
(16) Brooks, B. R.; Bruccoleri, R. E.; Olason, B. D.; States, D. J.; Swaminathan, S.; Karplus, M. *J. Comput. Chem.* **1983**, *4*, 187−217.
(17) Simonson, T.; Brünger, A. T. *J. Chem. Phys.* **1994**, *98*, 4683−4694.
(18) Smart, J. L.; Marrone, T. J.; McCammon, J. A. *J. Comput. Chem.* **1997**, *18*, 1750−1759.
(19) Kemp, B. E., Ed. *Peptides and Protein Phosphorylation*; CRC Press: Boca Raton, FL, 1990.
(20) Tholey, A.; Lindemann, A.; Kinzel, V.; Reed, J. *Biophys. J.* **1999**, *76*, 76−87.
(21) *Quanta98*; Molecular Simulations Inc.: San Diego, CA.
(22) Hoffmann, R.; Reichert, I.; Wachs, W. O.; Zeppezauer, M.; Kalbitzer, H.-R. *Int. J. Pept. Protein Res.* **1994**, *44*, 193−198.
(23) Gasteiger, J.; Marsili, M. *Tetrahedron* **1980**, *36*, 3219−3228.

Table 1. Peptides List

name	Pser	blocked[a]	deprotonated[b]	exp. condition
b0	no	yes	−	Ac-GSSS-NH_2 pH4.7
b1	yes	yes	single	Ac-GSSpS-NH_2 pH6.5
b2	yes	yes	double	Ac-GSSpS-NH_2 pH6.5
z0	yes	no	−	GSSS pH4.7
z1	yes	no	single	GSSpS pH4.7

[a] Our blocked tetrapeptide X has a form of Ac-X-$NHCH_3$. [b] The deprotonated state refers to the phosphoryl group if applicable.

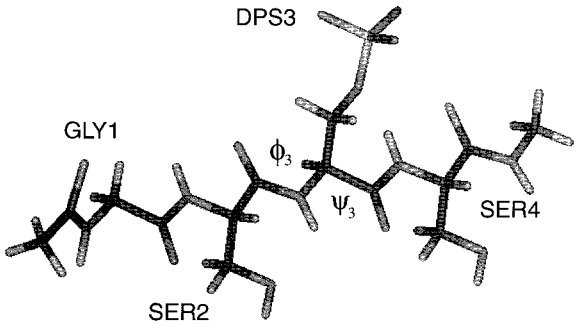

Figure 1. Starting structure of the totally deprotonated phosphorylated peptide GSS(p)S with blocked termini (b2).

To speed up conformational sampling, we carried out Brownian dynamics simulations at $T_i = 500$ K. We then used the histogram method[24] to obtain probability distribution and ensemble-averaged properties at $T_f = 283$ K at which the experimental measurements were made. In this work, we used the scaling weight $\exp[U(\{\vec{r}_j\})(1/k_B T_i - 1/k_B T_f)]$ for calculating ensemble-averaged properties.

Each peptide was simulated for 1 μs with the adaptive time step method using a normal time step of 10 fs and a small time step of 2.5 fs when the vdW energy of the current snapshot was larger than 17.5 kcal/mol. The choice of cutoff is based on the alanine tetrapeptide and other test systems of similar size. Choosing a lower cutoff would make the code use small time step more frequently and slow the calculation; a higher cutoff could risk instability. Each run took between 60 and 80 h on a Pentium III (500 MHz) Linux box.

IV. Results and Discussion

The free energy profiles are shown as Ramachandran maps of the middle serine of GSSS/GSS(p)S in Figure 2. Figure 2a shows that the terminally blocked unphosphorylated peptide strongly populates the C_{7eq} region (a region around $(\phi, \psi) = (-70°, 80°)$). However, as the peptide is phosphorylated, the α_R region (a region which forms the right α-helix structure, around $(-60°, -40°)$) is more populated than the C_{7eq} region (Figure 2b). This finding is a valuable complement to the experimental J coupling result. The latter is only sensitive to the backbone torsional angle ψ, but not to ϕ, which is critical to define the secondary structure. The doubly charged phosphorylated peptide, which can be found at high pHs, also samples the α_R region significantly, plus a nearby region around $\phi = -150°$, $\psi = -60°$ (Figure 2c). When the termini of the peptides were not blocked, the shift from C_{7eq} to α conformation upon phosphorylation was not observed in the simulations (Figure 2, d and e).

Table 2 shows some quantitative results. For the terminally blocked unphosphorylated peptide, the C_{7eq} conformation is more stable than the α form by 0.7 kcal/mol. When the peptide

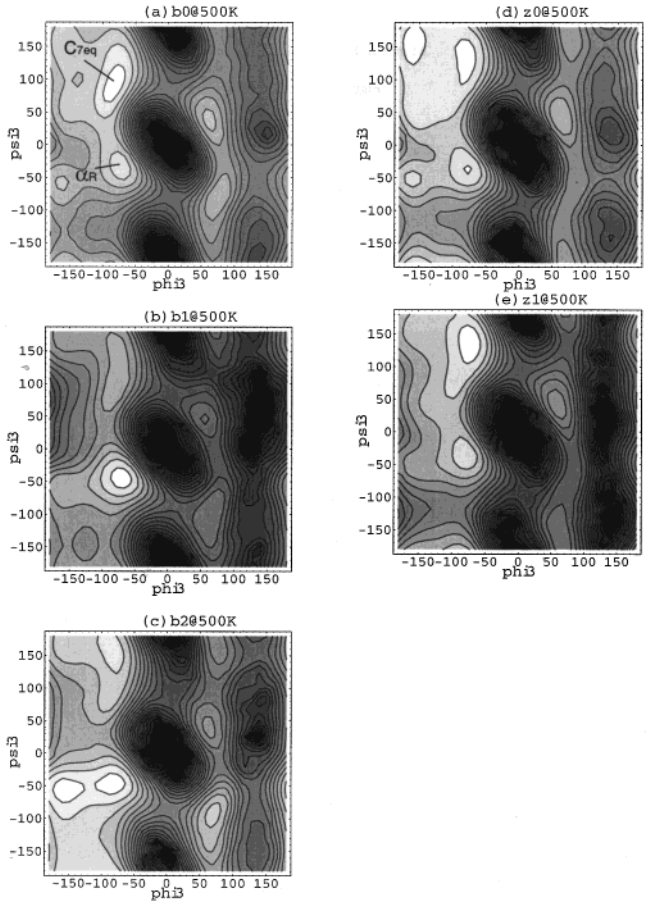

Figure 2. Conformational free energy shown as a function of the backbone torsional angles, ϕ and ψ of Ser3 at 500 K for b0 (a), b1 (b), b2 (c), z0 (d), and z1 (e). Gray levels were used to indicate free energy values, darker indicates a higher free energy. The brightest regions correspond to lowest values of free energy and are most heavily sampled.

is phosphorylated, this order is reversed, and the α form is more stable than that of the C_{7eq} by 2 kcal/mol. The helicity of the first serine along the peptide chain is also increased by phosphorylation. The doubly charged form, which occurs at high pH, also favors the helical state. The above free energy differences were calculated at 500 K. We used 500 K instead of 283 K because the results at 500 K give smoother-looking free energy maps, while the results at 283 K are rougher, making it difficult to identify peak positions and free energy differences between peaks. But from the results for the probability density function (PDF) below, it is easy to see that qualitatively the same conclusion holds for the room-temperature case.

The Karplus equation[25] is an empirical relation for connecting the magnitude of the spin−spin coupling constant $^3J(H_N H_\alpha)$ with the dihedral angle θ (H_N-N−C_α−H_α) as $^3J = F(\theta) \equiv A \cos^2\theta + B \cos\theta + C$. The parameters for the Karplus relation can be fitted from NMR and crystallographic data of proteins.[26] Theoretical results from quantum chemistry calculations of simple peptides[27] agree qualitatively with those obtained from the Karplus equation whose parameters were derived from proteins.

Since small peptides are flexible in solution, we calculated the ensemble average of ^3J as a functional of the probability

(24) Ferrenberg, A. M.; Swendsen, R. H. *Phys. Rev. Lett.* **1988**, *61*, 2635−2638.
(25) Karplus, M. *J. Phys. Chem.* **1959**, *30*, 11−15.
(26) Vuister, G. W.; Bax, A. *J. Am. Chem. Soc.* **1993**, *115*, 7772−7777.
(27) Malkin, V. G.; Malkin, O. L.; Eriksson, L. A.; Salahub, D. R. In *Modern Density Functional Theory: A Tool for Chemistry*; Seminario, J. M., Politzer, P., Eds.; Elsevier: New York, 1995.

Table 2. Comparison of Peptide Conformational Properties at 500 K

peptide (residue)	C_{7eq} peak(s)[a]	α peak(s)	$\Delta G_{C7eq\rightarrow\alpha}$ (kcal/mol)
b0 Gly1	(−85.0, 80.2)	(−75.0, −39.9)	0.889
Ser2	(−85.0, 80.1)	(−74.9, −40.1)	0.406
Ser3	(−85.0, 80.2)	(−75.1, −35.2)	0.669
Ser4	(−85.0,120)/(−160,140)	(−80, −45)	0.683/0.717
b1 Gly1	(−84.9 90.0)	(−80, 60)	−0.141
Ser2	(−157.5, 40.2)	(−79.8, −37.5)	−0.577
Ser(p)3	(−82.5, 87.6)	(−75.0, 45.3)	−1.98
Ser4	(−94.7, 70.3)	(−80, −35)/(−160, −55)	0.523/0.612
b2Gly1	(−177.6, 50.1)	(−177.6, −69.8)	−0.902
Ser2	(−155.2, 35.0)	(−85, −42)/(−160, −48)	0.08/0.08
Ser(p)3	(−82.9, 149.9)	(−155.0, −60)/(−85, −50)	−0.71/−0.64
Ser4	(−100, 40)/(−150, 35)	(−84.9, −14.6)	0.594/0.518
z0 Gly1	−	−	−
Ser2	(−82.5, 87.6)	(−74.7, −44.9)	0.736
Ser3	(−160, 145.1)/(80, 125)	(−82.4, −40.2)	0.328
Ser4	−	−	−
z1 Gly1	−	−	−
Ser2	(−94.9, 65.0)	(−75.3, −39.6)	0.551
Ser(p)3	(−75.0, 125.1)	(−82.4, −40.0)	0.63
Ser4	−	−	−

[a] Here, the C_{7eq} region refers to the region of the whole up-left quadrant of Ramachandran map ($\phi < 0$ and $\psi > 0$); α_R region of $\phi < 0$ and $\psi < 0$.

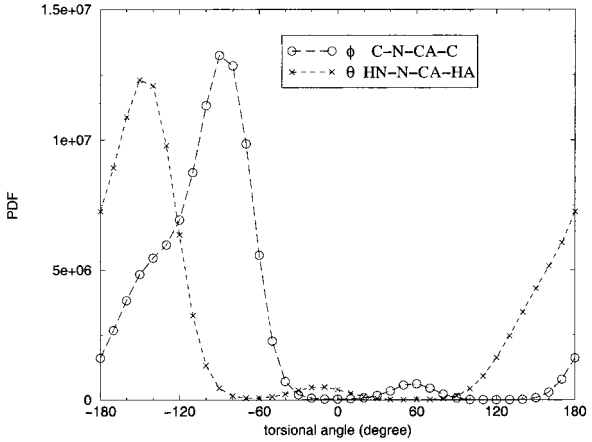

Figure 3. Probability density functions (PDFs) of θ and ϕ. The data were recorded from the 1 μs run of b1. They show that θ and ϕ approximately differ by a phase shift of 60°.

distribution of the torsional angle θ

$$\langle {}^3J\rangle = \frac{\int F(\theta)p(\theta)\mathrm{d}\theta}{\int p(\theta)\mathrm{d}\theta} \tag{5}$$

for comparison with corresponding experimental data. In our calculations, θ was obtained from ϕ as $\theta = \phi - 60$. This expression is commonly used in relating measured ^3J with ϕ obtained from crystal structures of proteins such as in the fitting of the parameters of the Karplus equation. Figure 3 shows that the $\theta = \phi - 60$ approximation is quite good. We also collected the torsional angles θ and calculated ^3J directly using them (data not shown). The results are similar to those results obtained by converting observed ϕ to θ as shown below.

Table 3 compares the calculated and experimental ^3J at 283 K. The results for the unphosphorylated peptide (b0) agree well with experiments.[20] All of the computed ^3J coupling constants except that of Gly1 are within 0.1 Hz of their corresponding experimental values. Gly1 shows a slightly larger discrepancy between computed and experimental results, but the difference is only 0.2 Hz, which is within the error bars of the calculated

Table 3. Comparison of Calculated and Experimental ^3J at 283 K

peptide (residue)	theor $^3J^a$	theor $^3J^b$	exptl ^3J (Hz, ±0.12)[c]
b0 Gly1	6.259	5.973	5.6/5.81
Ser2	6.464	6.705	6.72
Ser3	6.648	6.851	6.83
Ser4	6.772	7.078	7.14
b1 Gly1	6.182	6.140	5.74/?
Ser2	6.693	6.960	6.66
Ser(p)3	5.363	5.659	6.48
Ser4	7.464	7.639	7.3
b2 Gly1	5.952	6.132	(5.63/6.43)
Ser2	7.148	7.489	6.65
Ser(p)3	6.440	6.762	5.84
Ser4	6.826	6.901	6.93

[a] $A = 6.7/B = 1.3/C = 1.5$, Ludvigsen, S.; Andersen, K. V.; Poulsen, F. M. *J. Mol. Biol.* **1991**, *217*, 731−736. [b] $A = 6.51/B = -1.76/C = 1.60$, Vuister, G. W.; Bax, A. *J. Am. Chem. Soc.* **1993**, *115*, 7772−7777. [c] Tholey, A.; Lindemann, A.; Kinzel, V.; Reed, J. *Biophys. J.* **1999**, *76*, 76−87.

and experimental results. We chose the experimental data at pH 4 for comparing with the simulated results for the singly charged phosphorylated peptide (b1) because this form should dominate at this pH according to the pK_a of phosphoserine. The agreement between simulated and experimental results is still good although less so than for the unphosphorylated form. In particular, the computed ^3J value for the phosphorylated serine differs from the experimental value by 0.8 Hz, but both experiment and simulation agree on the negative shift of ^3J upon phosphorylation of serine. The approximate distance-dependent dielectric model may not be able to describe the electrostatic effects as well for this charged system compared to the neutral terminally blocked nonphosphorylated peptide. The agreement between simulated and experimental results for the doubly charged phosphorylated peptide (b2) deteriorates further. This could also result from the inadequacy of the distance-dependent dielectric model in describing electrostatics effects. In addition, the experimental data of the phosphorylated peptides are very sensitive to the pH value, and at pH 6.5, the contribution from the singly charged form is also significant.

Figure 4 shows the PDF of conformation of Ser3 before and after the corrections to 283 K by the histogram method, which

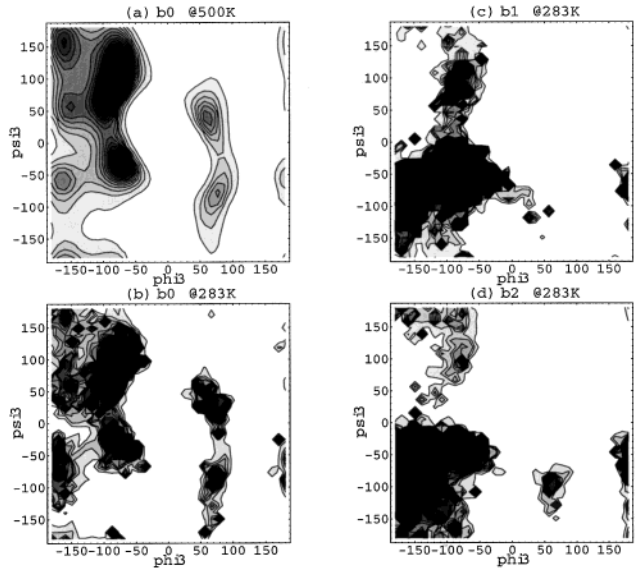

Figure 4. Probability density function (PDF) of conformation of Ser3 shown as a function of the backbone torsional angles ϕ and ψ. Darker indicates a higher value. The darkest are the highest probability regions. (a) and (b) show the changes of the PDF of b0 from 500 K to 283 K using the histogram method. (c) and (d) are the PDFs at 283K for b1 and b2.

leave a rougher landscape. We used the PDF results for 283 K to calculate ^3J in Table 3.

It is interesting to know whether the conformational change of peptide phosphorylation results from electrostatic or steric effect. To answer this question, we also did some test with setting charges of all the side chain atoms of residue 3 to zero. The results show that electrostatic effect is important. Without it, the conformation of the third residue does not have as dramatic a shift from C_{7eq} to α_R. Instead, both conformations have similar populations (data not shown).

V. Concluding Remarks

An all-atom constrained BD simulation algorithm has been implemented into the program UHBD[6] and tested on simulating tetrapeptides. An adaptive time step approach was introduced to reduce computational costs by allowing large time steps to be used. Microsecond simulations at 500 K were demonstrated to sample the conformational space of the peptides well, and the resulting ensembles allowed equilibrium properties at lower temperatures to be estimated using the histogram method. The calculated spin−spin coupling constants agree reasonably well with experiments. This gives confidence on using the simulation results to deduce the conformational changes of the peptide upon phosphorylation. The present constrained BD algorithm using adaptive time step is about 10 times faster than a corresponding LD simulation.

Our simulations of the tetrapeptide GSSS and its phosphorylated peptide GSS(p)S show that phosphorylation shifts the conformational preference from the C_{7eq} region into the α_R region. This algorithm should be helpful to the study of the properties of other flexible peptides in solution generally.

Although a simple distance-dependent dielectric model was used in this initial development of the atomistic Brownian dynamics method, the quality of such calculations can be improved in the future by application of the generalized Born[28,29] or Poisson−Boltzmann[18] solvation models.

Acknowledgment. This work was supported in part by the NIH, NSF, and Howard Hughes Medical Institute. Molecular Simulation Inc. provided useful scientific software. We also thank A. L. Perryman, L. S. Canino, D. Morikis, and A. H. Elcock for helpful discussions.

JA010190T

(28) Tsui, V.; Case, D. A. *J. Am. Chem. Soc.* **2000**, *122*, 2489−2498.
(29) Dominy, B. N.; Brooks, C. L. *J. Phys. Chem. B* **1999**, *103*, 3765−3773.